

AN ALTERNATIVE TO THE Λ CDM MODEL: THE CASE OF SCALE INVARIANCE

ANDRE MAEDER

Geneva Observatory, University of Geneva
CH-1290 Sauverny, Switzerland
andre.maeder@unige.ch

ABSTRACT

The hypothesis is made that, at large scales where General Relativity may be applied, the empty space is scale invariant. This establishes a relation between the cosmological constant and the scale factor λ of the scale invariant framework. This relation brings major simplifications in the scale invariant equations for cosmology, which contain a new term, depending on the derivative of the scale factor, that opposes to gravity and produces an accelerated expansion. The displacements due to the acceleration term make a high contribution Ω_λ to the energy-density of the Universe, satisfying an equation of the form $\Omega_m + \Omega_k + \Omega_\lambda = 1$. The models do not demand the existence of unknown particles. There is a family of flat models with different density parameters $\Omega_m < 1$.

Numerical integrations of the cosmological equations for different values of the curvature and density parameter k and Ω_m are performed. The presence of even tiny amounts of matter in the Universe tends to kill scale invariance. The point is that for $\Omega_m = 0.3$ the effect is not yet completely killed. The models with non-zero density start explosively with first a braking phase followed by a continuously accelerating expansion. Several observational properties are examined, in particular the distances, the $m-z$ diagram, the Ω_m vs. Ω_λ plot. Comparisons with observations are also performed for the Hubble constant H_0 vs. Ω_m , for the expansion history in the plot $H(z)/(z+1)$ vs. redshift z and for the transition redshift from braking to acceleration. These first dynamical tests are satisfied by the scale invariant models, which thus deserve further studies.

Keywords: cosmology: theory – cosmology: dark energy

1. INTRODUCTION

The cause of the accelerating expansion of the Universe (Riess et al. 1998; Perlmutter et al. 1999) is a major scientific problem at present, see for example the reviews by Weinberg (1989), Peebles & Ratra (2003), Frieman et al. (2008), Feng (2010), Porter et al. (2011) and Solà (2013). Here, we explore whether scale invariance may bring something interesting in this context.

The laws of physics are generally not unchanged under a change of scale, a fact discovered by Galileo Galilei (Feynman 1963). The scale references are closely related to the material content of the medium. Even the vacuum at the quantum level is not scale invariant, since quantum effects produce some units of time and length. As a matter of fact, this point is a historical argument, already forwarded long time ago against Weyl's theory (Weyl 1923).

The empty space at macroscopic and large scales does not have any preferred scale of length or time. The key-hypothesis of this work, is that the empty space at large scales is scale invariant. The astronomical scales differ by an enormous factor from the nuclear scales where quantum effects intervene. Thus, in the same way as we may use the Einstein theory at large scales, even if we do not have a quantum theory of gravitation, we may consider that the large scale empty space is scale invariant even if this is not true at the quantum level. Indeed, the results of the models below will show that the possible cosmological effects of scale invariance tend to very rapidly disappear when some matter is present in the Universe (cf. Fig. 3). The aim of this paper is to carefully examine the implications of the hypothesis of scale invariance in cosmology, accounting in particular for the specific hypothesis of scale invariance of the empty space at large. This is in the line of the remark by Dirac (1973) that the equations expressing the basic laws of Physics should be invariant under the widest possible group of transformations. This is the case of the Maxwell equations of electrodynamics which in absence of charges and currents show the property of scale invariance. While scale invariance has often been studied in relation with possible variations of the gravitational constant G , we

emphasize that no such hypothesis is considered here.

In Sect. 2, we briefly recall the basic scale invariant field equations necessary for the present study and apply them to the empty space at large scales. In Sect. 3, we establish the basic equations of the scale invariant cosmology accounting for the properties of the empty space. We also examine the density and geometrical parameters. In Sect. 4, we present numerical results of scale invariant models for different curvature parameters k and density parameters, and we make some comparisons with Λ CDM models. In Sect. 5, we examine several basic observational properties of the models and perform some first comparisons with model independent observations. Sect. 6 briefly gives the conclusions.

2. THE HYPOTHESIS OF SCALE INVARIANCE OF THE EMPTY SPACE AND ITS CONSEQUENCES

2.1. Scale invariant field equations

Many developments on a scale invariant theory of gravitation have been performed by physicists like [Weyl \(1923\)](#), [Eddington \(1923\)](#), [Dirac \(1973\)](#), and [Canuto et al. \(1977\)](#). Here, we limit the recalls to the very minimum. In the 4-dimensional space of General Relativity (GR), the element interval ds'^2 writes $ds'^2 = g'_{\mu\nu} dx^\mu dx^\nu$, (symbols with a prime refer to the space of GR, which is not scale invariant). A scale (or gauge) transformation is a change of the line element, for example ds' , of the form,

$$ds' = \lambda(x^\mu) ds. \quad (1)$$

There, $ds^2 = g_{\mu\nu} dx^\mu dx^\nu$ is the line element in another framework, where we now consider scale invariance as a fundamental property in addition to general covariance, (the coordinate intervals are dimensionless). Parameter $\lambda(x^\mu)$ is the scale factor connecting the two line elements. There is a conformal transformation between the two systems,

$$g'_{\mu\nu} = \lambda^2 g_{\mu\nu}. \quad (2)$$

The Cosmological Principle demands that the scale factor only depends on time. Scalars, vectors or tensors that transform like

$$Y'_\mu{}^\nu = \lambda^n Y_\mu{}^\nu, \quad (3)$$

are respectively called coscalars, covectors or cotensors of power n . If $n = 0$, one has an inscalar, invector or intensor, such objects are invariant to a scale transformation like (1). Scale covariance refers to a transformation (3) with powers n different from zero, while we reserve the term scale invariance for cases with $n = 0$. An extensive cotensor analysis has been developed by the above mentioned authors, see also [Bouvier & Maeder \(1978\)](#). The derivative of a scale invariant object is not in general scale invariant. Thus, scale covariant derivatives of the first and second order have been developed preserving scale covariance. Modified Christoffel symbols, Riemann-Christoffel tensor $R'_{\mu\lambda\rho}$, its contracted form $R'_\mu{}^\nu$ and the total curvature R also have their scale invariant corresponding terms which were developed and studied by [Weyl \(1923\)](#), [Eddington \(1923\)](#), [Dirac \(1973\)](#) and [Canuto et al. \(1977\)](#). The last reference provides a summary of scale invariant tensor analysis. The main difference with standard tensor analysis is that all these "new" expressions contain terms depending on κ_ν , which is a derivative of the above scale factor λ ,

$$\kappa_\nu = -\frac{\partial}{\partial x^\nu} \ln \lambda. \quad (4)$$

This term is called the coefficient of metrical connection. It is as a fundamental quantity as are the $g_{\mu\nu}$ in GR. We jump straightforward to the expressions of the contracted form $R'_\mu{}^\nu$ of the Riemann-Christoffel, derived by [Eddington \(1923\)](#) and [Dirac \(1973\)](#) in the scale invariant system,

$$R'_\mu{}^\nu = R''_{\mu}{}^\nu - \kappa_{\mu}{}^{\nu}{}_{;\mu} - \kappa_{\mu}{}^{\nu}{}_{;\mu} - g'_{\mu}{}^{\nu}{}_{;\alpha} \kappa^{\alpha} - 2\kappa_{\mu} \kappa^{\nu} + 2g'_{\mu}{}^{\nu} \kappa^{\alpha} \kappa_{\alpha}. \quad (5)$$

There, $R''_{\mu}{}^{\nu}$ is the usual expression in the Riemann geometry. We see that the additional terms with respect to GR are all only depending on κ_ν (which is also the case for the general field equation below). A sign ";" indicates a derivative with respect to the mentioned coordinate. The total curvature R in the scale invariant system is

$$R = R' - 6\kappa_{;\alpha}{}^{\alpha} + 6\kappa^{\alpha} \kappa_{\alpha}. \quad (6)$$

There, R' is the total curvature in Riemann geometry. The above expressions allow one to write the general scale invariant field equation ([Canuto et al. 1977](#)),

$$R'_{\mu\nu} - \frac{1}{2} g_{\mu\nu} R' - \kappa_{\mu;\nu} - \kappa_{\nu;\mu} - 2\kappa_{\mu} \kappa_{\nu} + 2g_{\mu\nu} \kappa_{;\alpha}{}^{\alpha} - g_{\mu\nu} \kappa^{\alpha} \kappa_{\alpha} = -8\pi G T_{\mu\nu} - \lambda^2 \Lambda_{\text{E}} g_{\mu\nu}, \quad (7)$$

where G is the gravitational constant (taken here as a true constant) and Λ_E the Einstein cosmological constant. The second member of (7) is scale invariant, as is the first one. This means that

$$T_{\mu\nu} = T'_{\mu\nu}. \quad (8)$$

This has further implications, as illustrated in the case of a perfect fluid by [Canuto et al. \(1977\)](#). The tensor $T_{\mu\nu}$ being scale invariant, one may write $(p + \varrho)u_\mu u_\nu - g_{\mu\nu}p = (p' + \varrho')u'_\mu u'_\nu - g'_{\mu\nu}p'$. The velocities u'^μ and u'_μ transform like

$$u'^\mu = \frac{dx^\mu}{ds'} = \lambda^{-1} \frac{dx^\mu}{ds} = \lambda^{-1} u^\mu, \\ \text{and } u'_\mu = g'_{\mu\nu} u'^\nu = \lambda^2 g_{\mu\nu} \lambda^{-1} u^\nu = \lambda u_\mu. \quad (9)$$

Thus, the energy-momentum tensor transforms like

$$(p + \varrho)u_\mu u_\nu - g_{\mu\nu}p = (p' + \varrho')\lambda^2 u_\mu u_\nu - \lambda^2 g_{\mu\nu}p'. \quad (10)$$

This implies the following scaling of p and ϱ in the new general coordinate system

$$p = p' \lambda^2 \quad \text{and} \quad \varrho = \varrho' \lambda^2. \quad (11)$$

Pressure and density are therefore not scale invariant, but are so-called coscalars of power -2. The term containing the cosmological constant now writes $-\lambda^2 \Lambda_E g_{\mu\nu}$, it is thus also a cotensor of power -2. To avoid any ambiguity, we keep all expressions with Λ_E , the Einstein cosmological constant, so that in the basic scale invariant field equation (7), it appears multiplied by λ^2 .

2.2. Application to the empty space

We now consider the application of the above scale invariant equations to the empty space. In GR, the corresponding $g'_{\mu\nu}$ represent the de Sitter metric for an empty space with Λ_E different from zero. The de Sitter metric can be written in various ways. An interesting form originally found by Lemaitre and by Robertson ([Tolman 1934](#)) is

$$ds'^2 = dt^2 - e^{2kt} [dx^2 + dy^2 + dz^2], \quad (12)$$

with the prime referring to the system of GR. In this form, the $g'_{\mu\nu}$ are not independent of the time coordinate. Also, we have $k^2 = \Lambda_E/3$ and $c = 1$. Now, a transformation of the coordinates can be made ([Mavrides 1973](#)),

$$\tau = \int e^{\left(-\sqrt{\frac{\Lambda_E}{3}} t\right)} dt, \quad (13)$$

where τ is a new time coordinate. This allows one to show that the de Sitter metric is conformal to the Minkowski metric. With the above transformation, the de Sitter line element ds'^2 may be written

$$ds'^2 = e^{\psi(\tau)} [d\tau^2 - (dx^2 + dy^2 + dz^2)], \quad \text{with } e^{\psi(\tau)} = e^{\left(2\sqrt{\frac{\Lambda_E}{3}} \tau\right)}. \quad (14)$$

From this and relation (13), we also have

$$e^{\psi(\tau)} = \frac{3}{\Lambda_E \tau^2}. \quad (15)$$

Thus, the corresponding line element in the scale invariant system can be written

$$ds^2 = \lambda^{-2} ds'^2 = \frac{3 \lambda^{-2}}{\Lambda_E \tau^2} [c^2 d\tau^2 - (dx^2 + dy^2 + dz^2)]. \quad (16)$$

Thus, the de Sitter metric is conformal to the Minkowski metric. Furthermore, if the following relation happens to be valid,

$$\frac{3 \lambda^{-2}}{\Lambda_E \tau^2} = 1, \quad (17)$$

then the line-element for the empty scale invariant space would just be given by the Minkowski metric,

$$ds^2 = d\tau^2 - (dx^2 + dy^2 + dz^2). \quad (18)$$

Now, we take as a hypothesis that the Minkowski metric (18) which characterizes Special Relativity also applies in the scale invariant framework. However, we have to check whether this hypothesis is consistent, *i.e* whether the Minkowski

metric is a choice permitted by the scale invariant field equation (7), and also whether relation (17) is consistent. The Minkowski metric implies that in (7) one has,

$$R'_{\mu\nu} - \frac{1}{2} g_{\mu\nu} R' = 0 \quad \text{and} \quad T'_{\mu\nu} = 0. \quad (19)$$

Thus, only the following terms are remaining from the above equation (7),

$$\kappa_{\mu;\nu} + \kappa_{\nu;\mu} + 2\kappa_{\mu}\kappa_{\nu} - 2g_{\mu\nu}\kappa_{;\alpha}^{\alpha} + g_{\mu\nu}\kappa^{\alpha}\kappa_{\alpha} = \lambda^2 \Lambda_E g_{\mu\nu}. \quad (20)$$

We are left with a relation between some functions of the scale factor λ (through the κ -terms (4)), the $g_{\mu\nu}$ and the Einstein cosmological constant Λ_E , which now appears as related to the properties of scale invariance of the empty space. Since λ may only be a function of time (which we now call t instead of τ), only the zero component of κ_{μ} is non-vanishing. Thus, the coefficient of metrical connection becomes

$$\kappa_{\mu;\nu} = \kappa_{0;0} = \partial_0 \kappa_0 = \frac{d\kappa_0}{dt} \equiv \dot{\kappa}_0. \quad (21)$$

The 0 and the 1, 2, 3 components of what remains from the field equation (20) become respectively

$$3\kappa_0^2 = \lambda^2 \Lambda_E, \quad (22)$$

$$2\dot{\kappa}_0 - \kappa_0^2 = -\lambda^2 \Lambda_E. \quad (23)$$

From (4), one has $\kappa_0 = -\dot{\lambda}/\lambda$ (with $c = 1$ at the denominator), thus (22) and (23) lead to

$$3 \frac{\dot{\lambda}^2}{\lambda^2} = \lambda^2 \Lambda_E \quad \text{and} \quad 2 \frac{\ddot{\lambda}}{\lambda} - \frac{\dot{\lambda}^2}{\lambda^2} = \lambda^2 \Lambda_E. \quad (24)$$

These expressions may also be written in equivalent forms

$$\frac{\ddot{\lambda}}{\lambda} = 2 \frac{\dot{\lambda}^2}{\lambda^2}, \quad \text{and} \quad \frac{\ddot{\lambda}}{\lambda} - \frac{\dot{\lambda}^2}{\lambda^2} = \frac{\lambda^2 \Lambda_E}{3}. \quad (25)$$

The first relation of (25) places a constraint on $\lambda(t)$. Considering a solution of the form $\lambda = a(t - b)^n + d$, we get $d = 0$ and $n = -1$. There is no condition on b , which means that the origin b of the timescale is not determined by the above equations. (The origin of the time will be determined by the solutions of the equations of the particular cosmological model considered, see Sect. 4). With the first of equations (24), we get

$$\lambda = \sqrt{\frac{3}{\Lambda_E}} \frac{1}{ct}. \quad (26)$$

For numerical estimates, c is indicated here. This condition is the same as (17) obtained from the above conformal transformation. We have thus verified that the Minkowski metric is compatible with the scale invariant field equation for the above condition.

The problem of the cosmological constant in the empty space is not a new one. First, in the context of RG, models with a non-zero cosmological constant, such as the Λ CDM models, do not admit the Minkowski metric, which may be a problem. Here, one can also consistently apply Special Relativity (with the Minkowski metric), even if the cosmological constant Λ_E is not equal to zero. Also Bertotti et al. (1990) are quoting the following remark they got from Bondi: “*Einstein’s disenchantment with the cosmological constant was partially motivated by a desire to preserve scale invariance of the empty space Einstein equations*”. This remark is consistent with the fact that Λ_E is not scale invariant as shown by the fact that Λ_E is multiplied by λ^2 in (7). Thus, the scale invariant framework offers a possibility to conciliate the existence of Λ_E with the scale invariance of the empty space.

3. COSMOLOGICAL EQUATIONS AND THEIR PROPERTIES

3.1. Basic scale invariant cosmological equations

The metric appropriate to cosmological models is the Robertson-Walker metric, characteristic of the homogeneous and isotropic space. We need to obtain the differential equations constraining the expansion factor $R(t)$ in the scale invariant framework. These equations can be derived in various equivalent ways (Canuto et al. 1977): – by expressing the general cotensorial field equation (7) with the Robertson-Walker metric, – by taking advantage that there is a conformal transformation between the metrics $g'_{\mu\nu}$ (GR) and $g_{\mu\nu}$ (scale invariant), – and by applying a scale

transformation to the current differential equations of cosmologies in $R(t)$. The scale invariant equations are,

$$\frac{8\pi G\varrho}{3} = \frac{k}{R^2} + \frac{\dot{R}^2}{R^2} + 2\frac{\dot{\lambda}\dot{R}}{\lambda R} + \frac{\dot{\lambda}^2}{\lambda^2} - \frac{\Lambda_E\lambda^2}{3} \quad (27)$$

$$-8\pi Gp = \frac{k}{R^2} + 2\frac{\ddot{R}}{R} + 2\frac{\ddot{\lambda}}{\lambda} + \frac{\dot{R}^2}{R} + 4\frac{\dot{R}\dot{\lambda}}{R\lambda} - \frac{\dot{\lambda}^2}{\lambda^2} - \Lambda_E\lambda^2. \quad (28)$$

These equations contain several additional terms with respect to the standard case. We now also account for expressions (24) and (25) for the empty space, which characterize λ and its properties. This is consistent with "the postulate of GR that gravitation couples universally to all energy and momentum" (Carroll et al. 1992). This also applies to the energy associated to the derivatives of λ in Eq. (27) and (28), which are responsible for an accelerated expansion as we will see below. Thus, with (24) and (25), the two above cosmological equations (27) and (28) nicely simplify to

$$\frac{8\pi G\varrho}{3} = \frac{k}{R^2} + \frac{\dot{R}^2}{R^2} + 2\frac{\dot{R}\dot{\lambda}}{R\lambda}, \quad (29)$$

$$-8\pi Gp = \frac{k}{R^2} + 2\frac{\ddot{R}}{R} + \frac{\dot{R}^2}{R^2} + 4\frac{\dot{R}\dot{\lambda}}{R\lambda}. \quad (30)$$

The combination of these two equations leads to

$$-\frac{4\pi G}{3}(3p + \varrho) = \frac{\ddot{R}}{R} + \frac{\dot{R}\dot{\lambda}}{R\lambda}. \quad (31)$$

Term k is the curvature parameter which takes values 0 or ± 1 , p and ϱ are the pressure and density in the scale invariant system. Einstein cosmological constant has disappeared due to the account of the properties of the empty space at large scales. These three equations differ from the classical ones, in each case only by an additional term containing $\frac{\dot{R}\dot{\lambda}}{R\lambda}$, which depends on time t . If $\lambda(t)$ is a constant, one gets the usual equations of cosmologies. Thus at any fixed time, the effects that do not depend on time evolution are just those predicted by GR (for example, the gravitational shift in stellar spectral lines). Significant departures from GR may appear in cosmological evolution over the ages.

What is the significance of the additional term? Let us consider (31): the term $\frac{\dot{R}\dot{\lambda}}{R\lambda}$ is negative, since according to (26) we have $\dot{\lambda}/\lambda = -\frac{1}{t}$. This term represents *an acceleration that opposes the gravitation*. The term $\frac{\dot{R}\dot{\lambda}}{R\lambda}$ is equal to $-\frac{H}{t}$. Thus, equations (29) to (31) are fundamentally different from those of the Λ CDM models: a variable term replaces the cosmological constant Λ_E . The new term implies that the acceleration of the expansion is variable in time, a suggestion which is not so new (Peebles & Ratra 1988). In this connexion, we note that the need to have a time-dependent term in order to satisfactorily interpret the recent observations has been recently emphasized by several authors, Sahni et al. (2014), Solá et al. (2015), Ding et al. (2015) and Solá et al. (2016).

3.2. The case of an empty Universe

Empty Universe models (like the de Sitter model) are interesting as they represent the asymptotic limit of models with lower and lower densities. Let us consider the case of a non-static scale invariant model with no matter and no radiation ($\varrho = 0$ and $p = 0$). The corresponding Friedman model would have an expansion given by $R(t) \sim t$ (with $k = -1$). In our case, expression (31) becomes simply

$$\frac{\ddot{R}}{R} = \frac{\dot{R}\dot{\lambda}}{R\lambda}. \quad (32)$$

The integration gives $\dot{R} = at$, where a is a constant, a further integration gives $R = a(t^2 - t_{\text{in}}^2)$. The initial instant t_{in} is chosen at the origin $R(t_{\text{in}}) = 0$ of the considered model. The value of t_{in} is not necessarily 0 and we do not know it yet. The model is non-static and the Hubble value at time t is

$$H = \frac{\dot{R}}{R} = 2\frac{t}{(t^2 - t_{\text{in}}^2)} \quad (33)$$

To get more information, we use Eq. (29) and get,

$$\dot{R}^2 t - 2\dot{R}R + kt = 0, \quad (34)$$

which leads to a second expression for H , $H = \frac{\dot{R}}{R} = \frac{1}{t} \pm \frac{\sqrt{1 - k\frac{t^2}{R^2}}}{t}$. For an empty model, we may take $k = -1$ or $k = 0$ (a choice consistent with (50) in the study of the geometrical parameters below). Let us first consider the case $k = -1$,

(the dimensions of k go like $[R^2/t^2]$). Fixing the scale so that $t_0 = 1$ and $R_0 = 1$ at the present time, we get (H_0 being positive),

$$H_0 = 1 + \sqrt{2}. \quad (35)$$

The above value (for $k = -1$) represents a lowest bound of H_0 -values to the models with non-zero densities, (since the steepness of $R(t)$ increases with higher densities according to (29)). In (35), H_0 is expressed as a function of $t_0 = 1$, however the value of H_0 should rather be expressed in term of the age $\tau = t_0 - t_{\text{in}}$ of the Universe in the considered model. We find t_{in} by expressing the equality of the two values of H_0 obtained above,

$$\frac{t_{\text{in}}}{t_0} = \sqrt{2} - 1. \quad (36)$$

This is the minimum value of t_{in} , (we notice that the scale factor $\lambda(t)$ at t_{in} has a value limited by $1 + \sqrt{2} = 2.4142$). The corresponding age τ becomes $\tau = (2 - \sqrt{2}) t_0$ and we may now express H_0 from (35) as a function of the age τ . We have quite generally, indicating here in parenthesis the timescale referred to,

$$\frac{H_0(\tau)}{\tau} = \frac{H_0(t_0)}{t_0}, \quad \text{thus } H_0(\tau) = H(t_0) \tau. \quad (37)$$

Thus, we get the following value of $H_0(\tau)$ (which appears as a maximum),

$$H_0(\tau) = \sqrt{2} \quad \text{for } k = -1. \quad (38)$$

Let us now turn to the empty model with $k = 0$. We have from what precedes $H_0 = 2$. As for $k = -1$, this value for the empty space is the minimum value of H_0 expressed in the scale with $t_0 = 1$. The comparison of this value and (33) leads to $t_{\text{in}} = 0$ and thus $\tau = t_0$. Here also, $t_{\text{in}} = 0$ is the minimum value for all models with $k = 0$ and thus τ is the longest age. We see that for $k = 0$, the scale factor λ of the empty space tends towards infinity at the origin. Expressing H_0 as a function of τ , we have $H_0(\tau) = 2$. Here also, $H_0(\tau)$ is an upper bound for the models with $k = 0$. On the whole, empty models, whether $k = -1$ or $k = 0$, obey very simple properties.

The empty scale invariant model expands like t^2 , faster than the linear corresponding Friedman model. The effects of scale invariance appear as the source of an accelerated expansion, consistently with the remark made about (31).

3.3. Critical density and Ω -parameters

We examine some general properties of the models based on equations (29) to (31). The critical density corresponding to the flat space with $k = 0$ is from (29) and $\lambda = 1/t$, with the Hubble parameter $H = \dot{R}/R$,

$$\frac{8\pi G \varrho_c^*}{3} = H^2 - 2 \frac{H}{t}. \quad (39)$$

We mark with a " * " this critical density that is different from the usual definition. The second member is always ≥ 0 , since the relative growth rate for non empty models is higher than t^2 . With (29) and (39), we have

$$\frac{\varrho}{\varrho_c^*} - \frac{k}{R^2 H^2} + \frac{2}{Ht} \left(1 - \frac{\varrho}{\varrho_c^*}\right) = 1. \quad (40)$$

$$\text{With } \Omega_{\text{m}}^* = \frac{\varrho}{\varrho_c^*}, \quad \text{and } \Omega_{\text{k}} = -\frac{k}{R^2 H^2}, \quad (41)$$

we get

$$\Omega_{\text{m}}^* + \Omega_{\text{k}} + \frac{2}{Ht} (1 - \Omega_{\text{m}}^*) = 1. \quad (42)$$

Consistently, $\Omega_{\text{m}}^* = 1$ implies $\Omega_{\text{k}} = 0$ and reciprocally. We also consider the usual definition of the critical density,

$$\Omega_{\text{m}} = \frac{\varrho}{\varrho_c} \quad \text{with} \quad \varrho_c = \frac{3H^2}{8\pi G}. \quad (43)$$

Between the two density parameters we have the relation

$$\Omega_{\text{m}} = \Omega_{\text{m}}^* \left(1 - \frac{2}{Ht}\right). \quad (44)$$

From (39) or (42), we obtain

$$\Omega_{\text{m}} + \Omega_{\text{k}} + \Omega_{\lambda} = 1, \quad \text{with} \quad \Omega_{\lambda} \equiv \frac{2}{Ht}. \quad (45)$$

The above relations are generally considered at time t_0 , but they are also valid at other epochs. The term Ω_λ arising from scale invariance has replaced the usual term Ω_Λ . The difference of the physical meaning is very profound. While Ω_Λ is the density parameter associated to the cosmological constant or to the dark energy, Ω_λ *expresses the energy density resulting from the variations of the scale factor*. This term does not demand the existence of unknown particles. It is interesting that an equation like (45) is also valid in the scale invariant cosmology.

While in Friedman's models there is only one model corresponding to $k = 0$, here for $k = 0$ there is a variety of models with different Ω_m and Ω_λ . For all models, whatever the k -value, the density parameter Ω_m remains smaller than 1, (this does not apply to Ω_m^* for $k = +1$). For $k = -1$ and $k = 0$, this is clear since $2t_0/H_0$ is always positive. For $k = +1$ (negative Ω_k), numerical models confirm that $\Omega_k + \Omega_\lambda$ is always positive so that $\Omega_m < 1$. Thus, a density parameter Ω_m always smaller than 1.0 appears as a fundamental property of scale invariant models.

3.4. The geometry parameters

We now consider the geometry parameters k , $q_0 = -\frac{\ddot{R}_0 R_0}{R_0^2}$ and their relations with Ω_m , Ω_k and Ω_λ at the present time t_0 . Expression (30), in absence of pressure and divided by H_0^2 , becomes

$$-2q_0 + 1 - \Omega_k = \frac{4}{H_0 t_0}. \quad (46)$$

Eliminating Ω_k between (46) and (42), we obtain

$$2q_0 = \Omega_m^* - \frac{2}{H_0 t_0}(\Omega_m^* + 1), \quad (47)$$

and thus, using Ω_m rather than Ω_m^* , we get

$$q_0 = \frac{\Omega_m}{2} - \frac{\Omega_\lambda}{2}. \quad (48)$$

This establishes a relation between the deceleration parameter q_0 and the matter content for the scale invariant cosmology. If $k = 0$, we have

$$q_0 = \frac{1}{2} - \Omega_\lambda = \Omega_m - \frac{1}{2}, \quad (49)$$

which provides a very simple relation between basic parameters. For $\Omega_m = 0.30$ or 0.20 , we would get $q_0 = -0.20$ or -0.30 . The above basic relations are different from those of the Λ CDM, which is expected since the basic equations (29) - (31) are different. Let us recall that in the Λ CDM model with $k = 0$ one has $q_0 = \frac{1}{2}\Omega_m - \Omega_\Lambda$. For $\Omega_m = 0.30$ or 0.20 , we get $q_0 = -0.55$ or -0.70 . In both cosmological models, one has simple, but different, relations expressing the q_0 parameter.

Let us now turn to the curvature parameter k . From the basic equation (29) and the definition of the critical density (39), this becomes,

$$\frac{k}{R_0^2} = H_0^2 \left[(\Omega_m^* - 1) \left(1 - \frac{2}{t_0 H_0} \right) \right], \quad (50)$$

which establishes a relation between k and Ω_m^* . It confirms that if $\Omega_m^* = 1$, one also has $k = 0$ and reciprocally. Values of $\Omega_m^* > 1$ correspond to a positive k -value, values smaller than 1 to a negative k -value. With Ω_m , one has

$$\frac{k}{R_0^2} = H_0^2 \left[\Omega_m - \left(1 - \frac{2}{t_0 H_0} \right) \right], \quad (51)$$

which is equivalent to (45) at time t_0 . We also have a relation between k and q_0 . From (47) and (50), we obtain

$$\frac{k}{R_0^2} = H_0^2 \left[2q_0 - 1 + \frac{4}{H_0 t_0} \right]. \quad (52)$$

For $k = 0$, it gives the same relation as (49) above. We emphasize that in all these expressions t_0 is not the present age of the Universe, but just the present time in a scale where $t_0 = 1$. As in Sect. 3.2, the present age is $\tau = t_0 - t_{in}$, where the initial time t_{in} depends on the considered model.

3.5. Inflexion point in the expansion

In the scale invariant cosmology, like in the Λ CDM models, there are both a braking force due to gravitation and an acceleration force. There may thus be initial epochs dominated by gravitational braking and other later epochs by acceleration. From (48), valid at any epoch t , we see that $q = 0$ occurs when

$$\Omega_m = \Omega_\lambda. \quad (53)$$

The gravitational term dominates in the early epochs and the λ -acceleration dominates in more advanced stages. The higher the Ω_m -value, the later the inflexion point occurs. The empty model (Sect. 3.2), where $R(t) \sim t^2$, is an exception showing only acceleration. For a flat model with $k = 0$, we have at the inflexion point when $\Omega_\lambda = \Omega_m = \frac{1}{2}$, the matter and the λ -contributions are equal and both equivalent to $1/2$. The inflexion points are identified for the flat models in Fig. 1 and Table 1. These results differ from those for the Λ CDM models. We have $q = 0$ for a flat Λ CDM model when $\frac{1}{2}\Omega_m = \Omega_\Lambda$. The acceleration term needs only to reach the half of the gravitational term to give $q = 0$, while in the scale invariant case the inflexion point is reached for the equality of the two terms.

3.6. Conservation laws

An additional invariance in the equations necessarily influences the conservation laws. Moreover, we have accounted for the scale invariance of the vacuum at macroscopic scales by using (24) and (25). These hypotheses have an impact on the conservation laws. We first rewrite (29) as follows and take its derivative,

$$8\pi G\rho R^3 = 3kR + 3\dot{R}^2 R + 6\frac{\dot{\lambda}}{\lambda}\dot{R}R^2, \quad (54)$$

$$\frac{d}{dt}(8\pi G\rho R^3) = -3\dot{R}R^2 \left[-\frac{k}{R^2} - \frac{\dot{R}^2}{R^2} - 2\frac{\ddot{R}}{R} - 2\frac{\ddot{R}}{R}\frac{\dot{\lambda}}{\lambda} - 2\frac{\ddot{\lambda}}{\lambda} - 4\frac{\dot{R}\dot{\lambda}}{R\lambda} + 2\frac{\dot{\lambda}^2}{\lambda^2} \right], \quad (55)$$

which contains many terms with λ and its derivatives. Eq. (29), (31) and (25) lead to many simplifications,

$$\frac{d}{dt}(8\pi G\rho R^3) = -3\dot{R}R^2 \left[8\pi Gp + \frac{R}{\dot{R}}\frac{\dot{\lambda}}{\lambda} \left(8\pi Gp + \frac{8\pi G\rho}{3} \right) \right], \quad (56)$$

$$3\lambda\rho dR + \lambda R d\rho + R\rho d\lambda + 3p\lambda dR + 3pR d\lambda = 0, \quad (57)$$

$$\text{and } 3\frac{dR}{R} + \frac{d\rho}{\rho} + \frac{d\lambda}{\lambda} + 3\frac{p}{\rho}\frac{dR}{R} + 3\frac{p}{\rho}\frac{d\lambda}{\lambda} = 0. \quad (58)$$

This can also be written in a form rather similar to the usual conservation law,

$$\frac{d(\rho R^3)}{dR} + 3pR^2 + (\rho + 3p)\frac{R^3}{\lambda}\frac{d\lambda}{dR} = 0. \quad (59)$$

These last two equations express the law of conservation of mass-energy in the scale invariant cosmology. For a constant λ , we evidently recognize the usual conservation law. We now write the equation of state in the general form, $P = w\rho$, with $c^2 = 1$, where w is taken here as a constant. The equation of conservation (58) becomes $3\frac{dR}{R} + \frac{d\rho}{\rho} + \frac{d\lambda}{\lambda} + 3w\frac{dR}{R} + 3w\frac{d\lambda}{\lambda} = 0$, with the following simple integral,

$$\rho R^{3(w+1)} \lambda^{(3w+1)} = \text{const.} \quad (60)$$

For $w = 0$, this is the case of ordinary matter of density ρ_m without pressure,

$$\rho_m R^3 \lambda = \text{const.} \quad (61)$$

which means that the inertial and gravitational mass (respecting the Equivalence principle) within a covolume should both slowly increase over the ages. We do not expect any matter creation as by Dirac (1973) and thus the number of baryons should be a constant. In GR, a certain curvature of space-time is associated to a given mass. Relation (61) means that the curvature of space-time associated to a mass is a slowly evolving function of the time in the Universe. For an empty model with $k = 0$, the change of λ would be enormous from ∞ at $t=0$ to 1 at t_0 . In a flat model with $\Omega_m = 0.30$, λ varies from 1.4938 at the origin to 1 at present. A change of the inertial and gravitational mass is not a new fact, it is well known in Special Relativity, where the effective masses change as a function of their velocity. In the standard model of particle physics, the constant masses of elementary particles originate from the interaction of the Higgs field (Higgs 2014; Englert 2014) in the vacuum with originally massless particles. Also in the Λ CDM, the

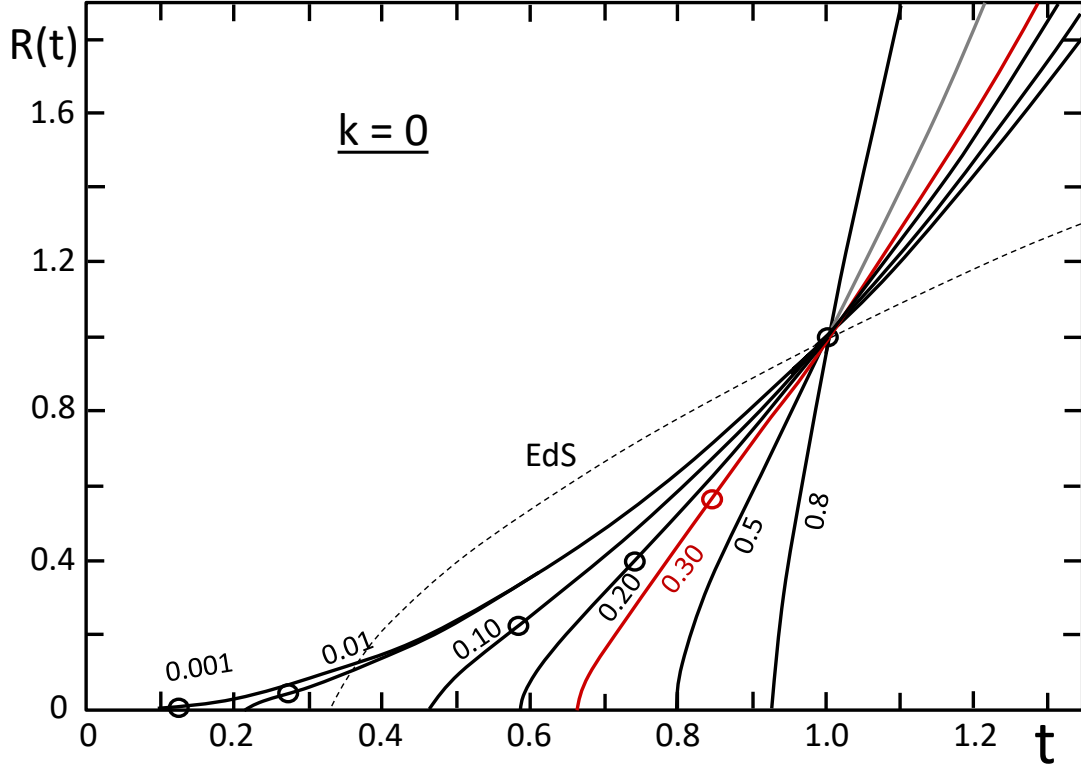


Figure 1. Some solutions of $R(t)$ for the models with $k = 0$. The curves are labeled by the values of Ω_m , the usual density parameter defined in (43). The Einstein-de Sitter model (EdS) is indicated by a dotted line. The small circles on the curves show the transition point between braking ($q > 0$) and acceleration ($q < 0$). For $\Omega_m = 0.80$, this point is at $R = 2.52$. The red curve corresponds $\Omega_m = 0.30$.

resulting acceleration of a gravitational system does not let its total energy unchanged (Krizek & Somer 2016). The assumption of scale invariance of the vacuum (at large scales) makes the inertial and gravitational masses to slowly slip over the ages, however by a rather limited amount in realistic models (see Fig. 3).

We check that the above expression (61) is fully consistent with the hypotheses made. According to (11), we have $\varrho' \lambda^2 = \varrho$, where the prime refers to the value in GR. Thus expression (61) becomes, also accounting for the scale transformation $\lambda R = R'$, $\varrho_m \lambda R^3 = \varrho'_m \lambda^3 R^3 = \varrho'_m R'^3 = \text{const}$. This is just the usual mass conservation law in GR.

Let us go on with the conservation law for relativistic particles and in particular for radiation with density ϱ_γ . We have $w = 1/3$. From (60), we get $\varrho_\gamma \lambda^2 R^4 = \text{const}$. As for the mass conservation, we may check its consistency with GR. This expression becomes $\varrho'_\gamma \lambda^4 R^4 = \text{const}$. and thus $\varrho'_\gamma R'^4 = \text{const}$. in the GR framework. Another case is that of the vacuum with density ϱ_v . It obeys to the equation of state $p = -\varrho$ with $c = 1$. Thus, we have $w = -1$ and from (60), $\varrho_v \lambda^{-2} = \text{const}$. indicating a decrease of the vacuum energy with time. With $\varrho'_v \lambda^2 = \varrho_v$, this gives $\varrho'_v = \text{const}$. in the GR framework, in agreement with the standard result. The above laws allow us to determine the time evolution of ϱ_m , ϱ_γ and temperature T in a given cosmological model, as shown in the next Section.

4. NUMERICAL COSMOLOGICAL MODELS

We now construct scale invariant cosmological models and examine their dynamical properties. The solutions of the equations are searched here for the case of ordinary matter with density ϱ_m and $w = 0$. We may write (29),

$$\frac{8\pi G \varrho_m R^3 \lambda}{3} = k R \lambda + \dot{R}^2 R \lambda + 2 \dot{R} R^2 \dot{\lambda}. \quad (62)$$

The first member is a constant. With $\lambda = t_0/t$ and the present time $t_0 = 1$, we have

$$\dot{R}^2 R t - 2 \dot{R} R^2 + k R t - C t^2 = 0, \quad \text{with } C = \frac{8\pi G \varrho_m R^3 \lambda}{3}. \quad (63)$$

Time t is expressed in units of $t_0 = 1$, at which we also assume $R_0 = 1$. The origin, the Big-Bang if any one, occurs when $R(t) = 0$ at an initial time t_{in} which is not necessarily 0 ($t_{\text{in}} = 0$ only for a flat empty model). We notice that

Table 1. Cosmological parameters of models with $k = 0$ and different Ω_m . $H_0(t_0)$ is the present Hubble constant in units of $t_0 = 1$, t_{in} is the time when $R(t) = 0$, $\tau = t_0 - t_{in}$ is the age of the Universe in units of $t_0 = 1$, $H_0(\tau)$ is the H_0 -value in units of τ , $t(q)$ and $R(q)$ are the values of t and R at the inflexion point, “ $H_{0\,obs}$ ” is the value of H_0 in $\text{km s}^{-1} \text{Mpc}^{-1}$.

Ω_m	C	$H_0(t_0)$	t_{in}	q_0	τ	$H_0(\tau)$	$t(q)$	$R(q)$	Ω_λ	$H_{0\,obs}$
0.001	0.0040	2.0020	0.0999	-0.50	0.9001	1.802	0.126	0.010	0.999	127.7
0.010	0.0408	2.0202	0.2154	-0.49	0.7846	1.585	0.271	0.047	0.990	112.3
0.100	0.4938	2.2222	0.4641	-0.40	0.5359	1.191	0.585	0.231	0.900	84.4
0.200	1.2500	2.5000	0.5848	-0.30	0.4152	1.038	0.737	0.397	0.800	73.5
0.250	1.7778	2.6667	0.6300	-0.25	0.3700	0.987	0.794	0.481	0.750	69.9
0.300	2.4490	2.8571	0.6694	-0.20	0.3306	0.945	0.843	0.568	0.700	66.9
0.400	4.4444	3.3333	0.7367	-0.10	0.2633	0.878	0.928	0.763	0.600	62.2
0.500	8.0000	4.0000	0.7936	0.00	0.2064	0.826	1.000	1.000	0.500	58.5
0.800	80	10	0.9282	0.30	0.0718	0.718	1.170	2.520	0.200	50.9
0.990	39600	200	0.9967	0.49	.00335	0.669	1.256	21.40	0.010	47.4

if we have a solution R vs. t , then (xR) vs. (xt) is also a solution. Thus, the solutions are also scale invariant, as expected from our initial assumptions.

Table 2. Data as a function of the redshift z for the models with $k = 0$ and $\Omega_m = 0.30$ (first six columns) and $\Omega_m = 0.20$ (last four columns). Columns 2 and 3 give R/R_0 and time t/t_0 ; column 4 contains the age in year with 13.8 Gyr at t_0 ; column 5 gives the Hubble parameter $H(t_0)$ in the scale $t_0 = 1$, while column 6 gives $H(z)$ in $\text{km s}^{-1} \text{Mpc}^{-1}$ for $\Omega_m = 0.30$. The last four columns give t/t_0 , the age also with 13.8 Gyr at t_0 , $H(t_0)$ and $H(z)$ for $\Omega_m = 0.20$.

z	R/R_0	t/t_0	age yr	$H(t_0)$	$H(z)$ obs	t/t_0	age yr	$H(t_0)$	$H(z)$ obs
Models with $\Omega_m = 0.30$					Models with $\Omega_m = 0.20$				
0.00	1	1	13.8E+09	2.857	67.0	1	13.8E+09	2.500	73.6
0.10	.9091	.9679	12.5E+09	3.088	72.3	.9631	12.6E+09	2.675	78.7
0.20	.8333	.9407	11.3E+09	3.324	77.9	.9316	11.5E+09	2.852	83.9
0.40	.7143	.8974	9.5E+09	3.810	89.3	.8806	9.8E+09	3.212	94.5
0.60	.6250	.8644	8.1E+09	4.321	101.2	.8412	8.5E+09	3.580	105.3
0.80	.5556	.8387	7.1E+09	4.852	113.7	.8099	7.5E+09	3.960	116.5
1.00	.5000	.8181	6.2E+09	5.408	126.7	.7845	6.5E+09	4.352	128.0
1.20	.4545	.8013	5.5E+09	5.987	140.2	.7636	5.9E+09	4.756	139.9
1.50	.4000	.7814	4.7E+09	6.895	161.5	.7383	5.1E+00	5.386	158.5
1.80	.3571	.7660	4.0E+09	7.854	184.0	.7184	4.4E+09	6.045	177.9
2.00	.3333	.7575	3.7E+09	8.522	199.6	.7074	4.1E+09	6.500	191.2
2.34	.2994	.7457	3.2E+09	9.698	227.1	.6918	3.6E+09	7.303	214.9
3.00	.2500	.7290	2.5E+09	12.16	284.6	.6694	2.8E+09	8.963	263.7
4.00	.2000	.7131	1.8E+09	16.24	380.5	.6476	2.1E+09	11.72	344.8
9.00	.1000	.6855	6.7E+08	42.46	994.5	.6085	7.9E+08	29.27	861.2

4.1. The case of a flat space ($k = 0$)

The case of the Euclidean space is evidently the most interesting one in view of the confirmed results of the space missions investigating the Cosmic Microwave Background (CMB) radiation with Boomerang (de Bernardis et al. 2000), WMAP (Bennett et al. 2003) and the Planck Collaboration (2014). Expression (63) becomes

$$\dot{R}^2 R t - 2 \dot{R} R^2 - C t^2 = 0. \quad (64)$$

For $t_0 = 1$ and $R_0 = 1$, with the Hubble constant $H_0 = \dot{R}_0/R_0$ at the present time, the above relation leads to $H_0^2 - 2 H_0 = C$. This gives $H_0 = 1 \pm \sqrt{1 + C}$, where we take the sign + since H_0 is positive. We now relate C to Ω_m

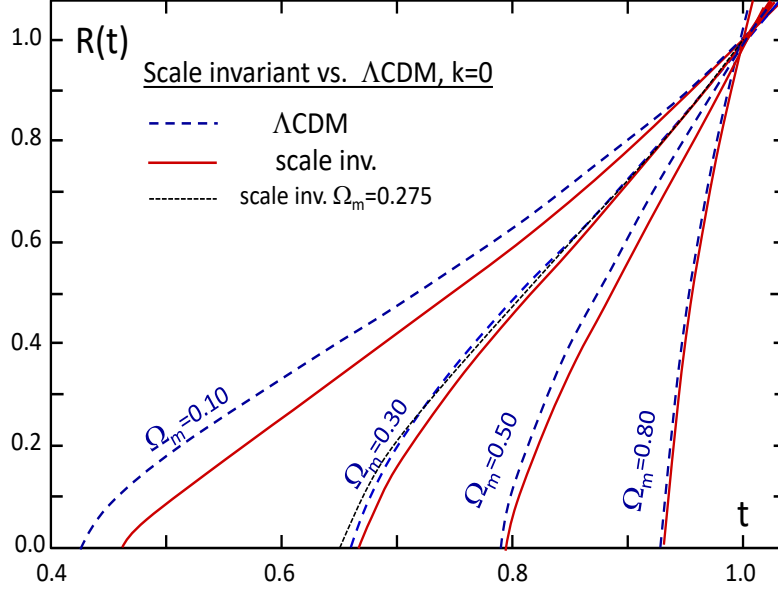


Figure 2. Comparisons of the $R(t)$ functions of the Λ CDM and scale invariant models for given values of Ω_m . As an example, the scale invariant model with $\Omega_m = 0.275$ lies very close to the Λ CDM model with $\Omega_m = 0.30$, but the slopes are always slightly different.

at time t_0 . We have $\Omega_m = 1 - \Omega_\lambda$ and thus from (45)

$$H_0 = \frac{2}{1 - \Omega_m}. \quad (65)$$

This gives H_0 (in unit of t_0) directly from Ω_m . We now obtain C as a function of Ω_m ,

$$C = \frac{4}{(1 - \Omega_m)^2} - \frac{4}{(1 - \Omega_m)} = \frac{4\Omega_m}{(1 - \Omega_m)^2}, \quad (66)$$

which allows us to integrate (64) for a chosen Ω_m (at present). As seen above, the scale invariant cosmology with $k = 0$, like the Λ CDM, but unlike the Friedman models, permits a variety of models with different Ω_m . This is an interesting property in view of the results on the CMB which support a flat Universe [Planck Collaboration \(2014\)](#). Eq.(66) shows that for Ω_m ranging from $0 \rightarrow 1$, C covers the range from 0 to infinity.

To integrate (64) numerically, we choose a present value for Ω_m , which determines C . We proceed to the integration backwards and forwards in time starting from $t_0 = 1$ and $R_0 = 1$. Table 1 gives some model data for different Ω_m . The integration provides $R(t)$ and the related parameters H and q . Fig. 1 shows some curves of $R(t)$ for different values of Ω_m . To get H_0 in $\text{km s}^{-1} \text{Mpc}^{-1}$, we proceed as follows. The inverse of the age of the Universe of 13.8 Gyr ([Frieman et al. 2008](#)) is $2.295 \cdot 10^{-18} \text{ s}^{-1}$, which in the units currently used is equal to $70.85 \text{ km s}^{-1} \text{Mpc}^{-1}$. This numerical value is to be associated to $H_0(\tau) = 1.000$ in column 7 of Table 1. On the basis of this correspondence, we multiply all values of $H_0(\tau)$ of column 7 by $70.85 \text{ km s}^{-1} \text{Mpc}^{-1}$ to get the values of H_0 in current units (last column). The Hubble constant $H_0 = 66.9 \text{ km s}^{-1} \text{Mpc}^{-1}$ is predicted for $\Omega_m = 0.30$ ($73.5 \text{ km s}^{-1} \text{Mpc}^{-1}$ for $\Omega_m = 0.20$). The agreement with recent values of H_0 (Sect. 5.4) indicates that the expansion rate is correctly predicted for the given age of the Universe.

The models of Fig. 1 show that after an initial phase of braking, there is an accelerated expansion, which goes on all the way. No curve $R(t)$ starts with an horizontal tangent, except the empty model, where the effect of scale invariance are the largest. All models with matter start explosively with very high values of $H = \dot{R}/R$ and a positive value of q , indicating braking. The locations of the inflexion points, where q changes sign, are indicated by a small open circle. For $\Omega_m \rightarrow 1$, the age of the Universe is smaller. At the same time for increasing Ω_m , $H_0(t_0)$ (in units of t_0) becomes much larger, while H_0 in units of τ and in $\text{km s}^{-1} \text{Mpc}^{-1}$ becomes smaller. In Table 2, we give some basic data for the reference models with $k = 0$ and $\Omega_m = 0.30$ and 0.20 as a function of the redshift z . The values of $H(z)$ in $\text{km s}^{-1} \text{Mpc}^{-1}$ are derived as for Table 1, by the relation $H(z) = 70.85 \cdot \tau(z = 0) \cdot H(t/t_0)$.

Fig. 2 shows the comparison of the scale invariant and Λ CDM models both with $k = 0$. The curves of both kinds of models are similar with smaller differences for increasing density parameters. The figure shows that the scale invariant

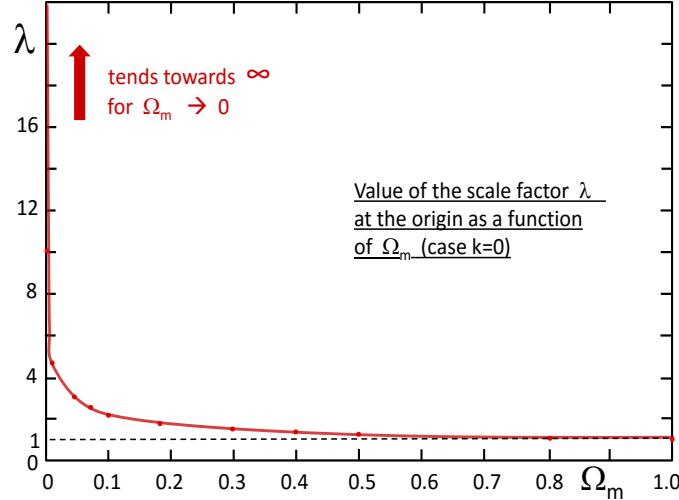


Figure 3. The scale factor λ at the origin $R(t) = 0$ for models with $k = 0$ and different Ω_m at present time t_0 . At t_0 , $\lambda = 1$ for all models. This curve shows that for increasing densities, the amplitudes of the variations of the scale factor λ are very much reduced.

model with $\Omega_m = 0.275$ lies very closely to the Λ CDM model with $\Omega_m = 0.30$ with values of $R(t)$ slightly smaller for $R(t) > 0.30$, and slightly larger for lower values. These results imply that for most observational tests the predictions of the scale invariant models are not far from those of the Λ CDM models.

The behavior of $\lambda(t)$ is interesting (Fig. 3). For an empty space, the factor λ varies enormously, between ∞ at the origin and 1 at present. As soon as matter is present, the range of λ -values falls dramatically. For $\Omega_m = 0.30$, λ varies only from 1.4938 to 1.0 between the Big-Bang and now. Thus, the presence of less than 1 H-atom per cubic meter is sufficient to drastically reduce the amplitude of the domain of λ -variations. For $\Omega_m \rightarrow 1$, the scale factor λ tends towards 1 all the way. This means that the effects of scale invariance disappear and that the cosmological solutions tend towards those of GR. Indeed, we have seen that there is no scale invariant solution for $\Omega_m > 1$. Thus, in the line of the remark by Feynman (1963) in the introduction, we see that the presence of even very tiny amounts of matter in the Universe tends to very rapidly kill scale invariance. The point is that with $\Omega_m \sim 0.30$, the effect appears to be not yet completely killed and may thus deserve the present investigation.

4.2. The elliptic and hyperbolic scale invariant models

Although the non-Euclidean models are not supported by the observations of the CMB radiation (Planck Collaboration 2014), we briefly present the main properties of these models. We first have to relate the constant C to the density parameters. Expressing C in (63) with (39) and (41), we get at time t_0

$$C = \frac{8\pi G \rho_m}{3} = \Omega_m^* H_0^2 \left(1 - \frac{2}{t_0 H_0}\right), \quad (67)$$

and with (44)

$$C = \Omega_m H_0^2. \quad (68)$$

We also have relation (50) between the geometrical parameter k and Ω_m^* at the present time. It allows us to eliminate $[1 - 2/(t_0 H_0)]$ from (67) and obtain

$$C = \frac{k \Omega_m^*}{\Omega_m^* - 1}, \quad \text{with } k = \pm 1. \quad (69)$$

A model is defined by its Ω_m^* -value at the present time. For integrating (63), we first choose an arbitrary value of Ω_m^* for the considered k and then use (69) to obtain the corresponding C -value. The integration of (63) from the present $t_0 = 1$ and $R_0 = 1$ is performed forwards and backwards to obtain $R(t)$ and its derivatives. The value of $H_0 = (\dot{R}/R)_0$ gives us the corresponding Ω_m . For non-zero curvature models, $\Omega_m \neq (1 - \Omega_\lambda)$ at all times and Ω_m^* is not equal to 1 as for $k = 0$. Ω_m^* like the other Ω -terms vary with time. Also, all models have $\Omega_m < 1$ (Sect. 3.3).

Figs. 4 illustrates some solutions for $k = \pm 1$. From these figures, we see that the three families of $R(t)$ curves for $k = 0$ and $k = \pm 1$ are on the whole not very different from each other. The curves for $k = \pm 1$ also show the same

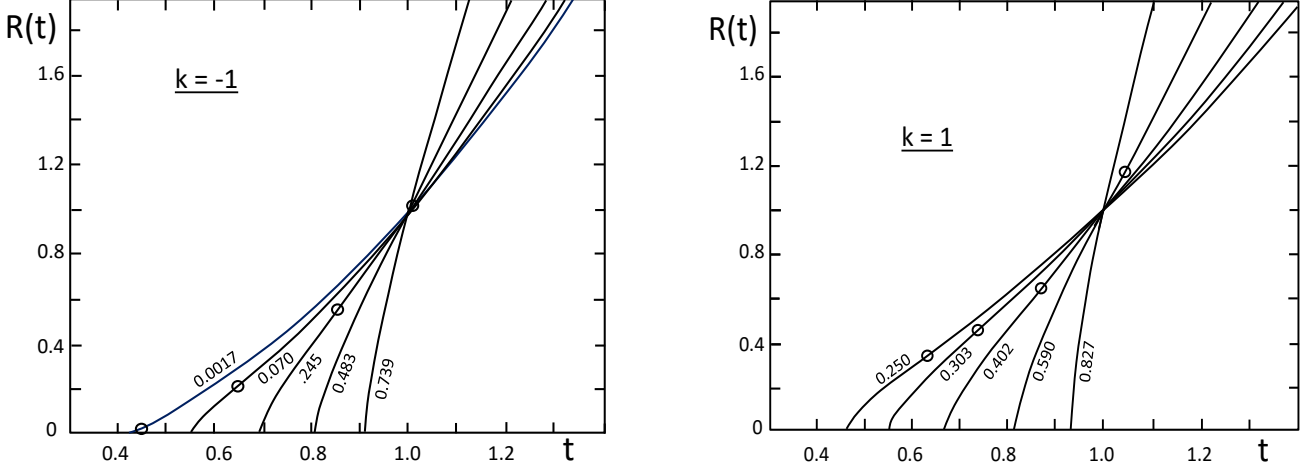


Figure 4. Left: Some solutions of $R(t)$ for the models with $k = -1$. The curves are labeled by the values of Ω_m (at t_0), the usual density parameter defined by (43). The corresponding values of Ω_m^* used to define C are 0.001, 0.315, 0.70, 0.90, 0.98 from left to right. Right: Some solutions of $R(t)$ for $k = +1$. The corresponding values of the usual density parameter Ω_m are indicated. The values of Ω_m^* used to define the C -values are 1000, 3.0, 1.5, 1.10, 1.01.

succession as for $k = 0$ with first a braking and then an acceleration phase. The relative similarity of the three families indicates that the curvature term k has a limited effect compared to the density (expressed by C in the equations) and to the acceleration resulting from scale invariance. Unlike in the Friedman models, the same density parameters Ω_m may exist for different curvatures.

The models with $k = -1$ (like for $k = 0$) have all possible values of C from 0 to infinity, while their usual density parameter Ω_m remains smaller than 1.0. For $k = +1$, we notice a peculiar behavior. When C increases from 1 to infinity, Ω_m^* decreases from infinity to 1.0, while Ω_m goes from a limit of 0.25 to 1.0. The opposite behavior of the two density parameters results from the fact that the term $[1 - 2/(t_0 H_0)]$ becomes very small. As an example, for $\Omega_m^* = 1000$, $H_0 = 2.00050$, so that the term $[1 - 2/(t_0 H_0)] = 0.00025$ and $\Omega_m = 0.25$.

5. SOME OBSERVATIONAL PROPERTIES OF SCALE INVARIANT MODELS

We examine several observational properties of scale invariant models to see whether there are some incompatibilities resulting from scale invariant models. We try to concentrate on a few tests where the observational data are not derived within some specific cosmological models.

5.1. Distances vs. redshift in scale invariant cosmology

Distances are essential to many cosmological tests. The distance of a given object of coordinate r_1 depends on the evolution of the expansion factor $R(t)$. Important distance definitions are those of the proper motion distance d_M , the angular diameter distance d_A and the luminosity distance d_L . They are related by

$$d_L = (1+z)d_M = (1+z)^2 d_A, \quad \text{with} \quad d_M = R_0 r_1, \quad (70)$$

The relations between these three distances are model independent. We have

$$R_0 r_1 = \frac{c}{H_0} \int_0^z \frac{dz}{H(z)}. \quad (71)$$

From (29), we may write

$$\frac{H^2(z)}{H_0^2} = \Omega_m(1+z)^3 t + \Omega_k(1+z)^2 + 2 \frac{H(z)}{H_0} \left(\frac{1}{H_0 t} \right), \quad (72)$$

where we ignore relativistic particles in the present matter-dominated era. Solving the above relation, we get

$$H(z) = \frac{1}{t} + \sqrt{\frac{1}{t^2} + H_0^2 [\Omega_m(1+z)^3 t + \Omega_k(1+z)^2]}, \quad (73)$$

where the sign "+" has been taken, since $H(z)$ is positive. This allows one to calculate the various distances (70) in the scale invariant framework. Below we examine carefully one of them, say the angular diameter distance $d_A = d_M/(1+z)$. Fig. 5 compares d_A for the scale invariant and Λ CDM models for $k = 0$ and $\Omega_m = 0, 0.1, 0.3, 0.99$. We see that:

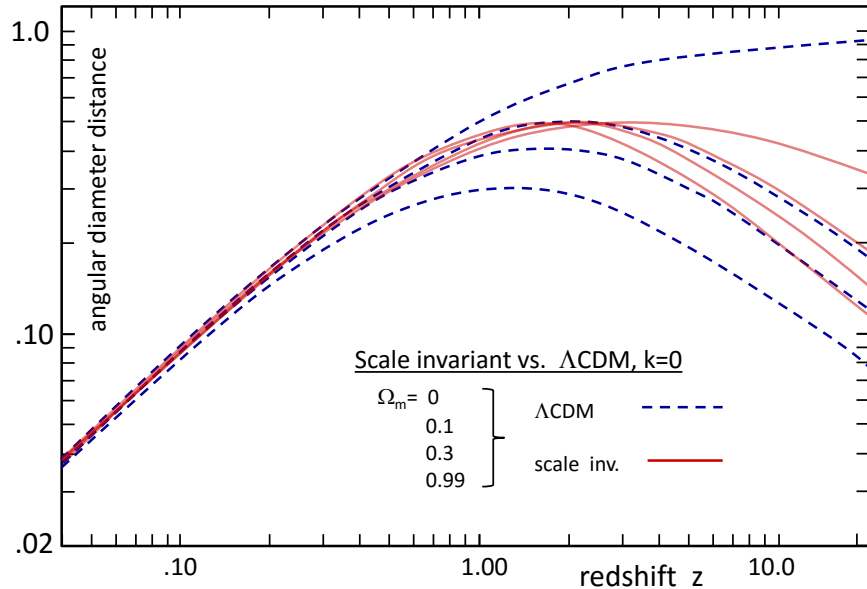


Figure 5. The angular diameter distance d_A vs. redshift z for flat scale invariant models (continuous red lines) compared to flat Λ CDM models (broken blue lines). The curves are given for $\Omega_m = 0, 0.1, 0.3, 0.99$, from the upper to the lower curve in both cases (at $z > 3$).

- Up to a redshift $z = 2$, the relations between d_A and z for scale invariant models are very close to each other whatever Ω_m , with a separation generally smaller than ~ 0.04 dex. At $z = 0.6$, for $\Omega_m = 0, 0.1, 0.3, 0.99$, one respectively has $\log d_A = -0.480, -0.467, -0.450, -0.437$. For $z = 1$, the corresponding values are $-0.383, -0.367, -0.349, -0.342$. Up to $z \approx 2$, higher density models lead to larger d_A , while above $z \approx 2$ this is the contrary. Then at $z = 2$, all curves converge, before slowly diverging for higher z . For Λ CDM models, higher density models have lower d_A with an always increasing separation between the curves.

- At redshift 1, the scale invariant models with $k = 0$ and Ω_m between 0 and 0.99 lie between the Λ CDM models with $\Omega_m = 0.1$ and 0.3, a trend supported by related tests.

- The above properties are evidently also shared by the proper motion distances, the luminosity distances, as well as by number counts (for $k = 0$ at least). This means that, if scale invariant cosmology applies, the cosmological tests based on the magnitude–redshift diagram, on the angular diameters, as well as on the number counts up to a redshift of about 2 will require very high precision data to determine Ω_m . A clear discrimination between the scale invariant and Λ CDM models from tests based on distance parameters likely requires redshifts higher than 2.

We note that at high z a fixed angular beam subtends a smaller scale object for lower density models, giving thus smaller microwave background fluctuations (Carroll et al. 1992). The differences are smaller in the scale invariant case compared to the Λ CDM model. Further works will explore such consequences.

5.2. The magnitude–redshift diagram

The magnitude–redshift diagram has been a major tool for the discovery of the accelerated expansion (Riess et al. 1998; Perlmutter et al. 1999). The flux f received from a distant standard candle, like a supernova of type Ia, with a luminosity L goes like $f = L/(4\pi d_L^2)$ and the distance modulus $m - M$ of a source of coordinate r_1 is

$$m - M = \text{const.} + 5 \log(R_0 r_1) + 5 \log(1 + z), \quad (74)$$

where $R_0 r_1$ is obtained from (71). We choose the constant so that $m - M = 33.22$ at redshift $z = 0.01$. Such an adjustment is based on the recent $m - M$ vs. z diagram from the joined analysis of type Ia supernovae observations obtained in the SDSS-II and SNLS collaborations given in Fig. 8 by Betoule et al. (2014). At this low redshift the various models, whether Λ CDM or scale invariant, give a similar value of the above constant. Relations $m - M$ vs. z are calculated for a few Λ CDM and scale invariant models for various Ω_m -values.

Fig. 6 shows some results in the $m - M$ vs. z plot. We notice a clear separation of the curves for the Λ CDM models, which were the basic reference suggesting the accelerated expansion. In agreement with the results for distances, we see that up to $z = 1$ (the present limit in such plots) the $m - M$ vs. z curves show very little dependence on Ω_m for

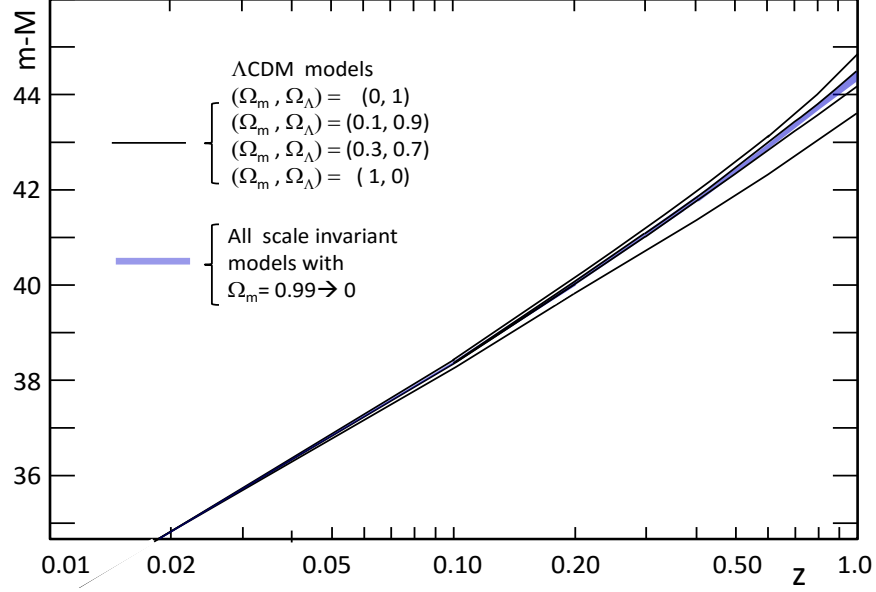


Figure 6. The magnitude-redshift diagram for some Λ CDM and scale invariant models for different values of Ω_m .

scale invariant models. Models with Ω_m between 0 and 0.99 are squeezed within the thin blue band of Fig. 6, which lies between the curves for $\Omega_m = 0.10$ and 0.30 of the Λ CDM models. In Fig. 6, the curves of the Λ CDM models with higher Ω_m are lower at all z (higher apparent brightness since smaller distance). This is also the case for scale invariant models with $z > 2$, but below this redshift the order is inverse with very small separations.

Our main purpose here is not to determine an accurate value of Ω_m in the scale invariant framework, but to see whether this theory clashes with current observations. Clearly from the above tests based on the distances, this is not the case. We note that in the framework of scale invariant models, it may be more difficult to assign a value of Ω_m than in the Λ CDM models due to the smaller effects of the density parameter. The $m - z$ diagram for scale invariant models shows curves which are not in contradiction with the current results for the Λ CDM models. These two kinds of models may support slightly different values of Ω_m .

5.3. The Ω_λ vs. Ω_m plot

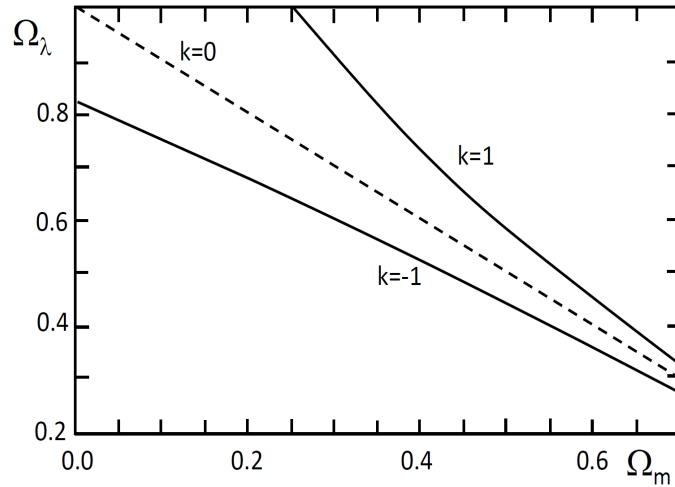


Figure 7. Plot of the density parameters Ω_λ vs. Ω_m for scale invariant models with $k = 0, \pm 1$

The Ω_m vs. Ω_m plot is a major tool in observational cosmology. Comparisons between the Λ CDM models and observational parameters have been performed, for example recently, by Reid et al. (2010), Betoule et al. (2014), the Planck Collaboration (2014). These comparisons clearly favor values of Ω_m around 0.30 and $\Omega_\lambda \approx 0.70$ in the Λ CDM models. The point is that the various analyses of observations, such as the $m - z$ diagram, the BAO oscillations and the CMB fluctuations, may lead to a slightly different value of Ω_m , when interpreted in the scale invariant models. From the same observations, different cosmological models lead to different values of the cosmological parameters.

Fig. 7 illustrates the relation between Ω_λ vs. Ω_m for the various k -values. The effect of different curvatures is larger for lower density parameters Ω_m . Flat models which are clearly supported by the CMB observations (de Bernardis et al. 2000; Bennett et al. 2003; Planck Collaboration 2014) lie on the diagonal line $\Omega_\lambda = 1 - \Omega_m$. This is the case for the preferred Λ CDM model (Betoule et al. 2014). The differences between the scale invariant and Λ CDM models being small (cf. Fig. 2, this is not the case for the EdS model in Fig. 1), the resulting point of the flat scale invariant models must lie not so far on the $k = 0$ diagonal.

5.4. The relation between H_0 , Ω_m and the age of the Universe

An important test independent on cosmological models is provided by the value of the Hubble constant H_0 . For a given age of the Universe, the value of H_0 in $\text{km s}^{-1} \text{Mpc}^{-1}$ depends on Ω_m , as shown by Table 1. Thus, for an age of the Universe of 13.8 Gyr (with some uncertainty limits), we get a constraint on Ω_m from the observed value of H_0 (Fig. 8).

There has always been some scatter in the results for H_0 , a scatter which has remarkably decreased with time. There is still today a bi-polarization in the results for H_0 , with on one side the values based on the distance ladder which support a value of H_0 around $73 \text{ km s}^{-1} \text{Mpc}^{-1}$. In particular, Frieman et al. (2008) gave a value $H_0 = 72 \pm 5$ (in the same units), Freedman & Madore (2010) obtained a value $H_0 = 73 \pm 2$ (random) ± 4 (systematic). Recently, Riess et al. (2016) proceeded to a new determination based on HST data and obtained $H_0 = 73.00 \pm 1.75$.

The above values appear as outliers when compared to the accumulation of lower values around $H_0 = 68 \text{ km s}^{-1} \text{Mpc}^{-1}$. Noticeably, the median of a collection of 553 determinations of the Hubble constant converges towards the low value, giving $H_0 = 68 \pm 5 \text{ km s}^{-1} \text{Mpc}^{-1}$ (Chen & Ratra 2011). Sievers et al. (2013) from high- ℓ data for the CMB power spectrum from the Atacama Cosmology Telescope combined with data from WMAP-7yr support a value $H_0 = 70 \pm 2.4$ within the Λ CDM model. This is consistent with the WMAP-9 yr value of $H_0 = 70.0 \pm 2.2$ (69.33 ± 0.88 when combined with BAO data) derived by Hinshaw et al. (2013). Also, the Planck Collaboration (2014) gives $H_0 = 67.3 \pm 1.2$ within the six-parameter Λ CDM cosmology. The combination of BAO and SN Ia data into an inverse distance ladder leads to a value $H_0 = 67.3 \pm 1.1$ (Aubourg et al. 2015). This value is independent on the Λ CDM model and rests only on the value of the standard ruler used in BAO analyses. This

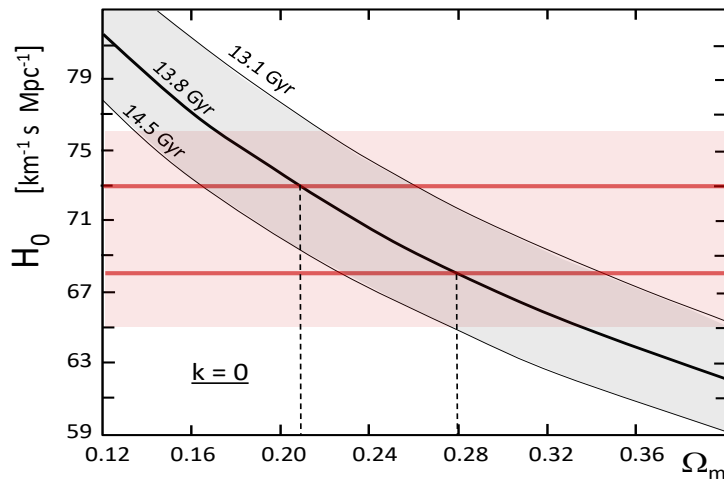


Figure 8. The relations between the Hubble constant and Ω_m for scale invariant models with $k = 0$ for three different values of the age of the Universe (continuous black lines), the grey hatched area covers the domain of these values corresponding to $\pm 5\%$ differences. The low and high values of H_0 discussed in the text are indicated with an uncertainty band (pink area) of $\pm 3 \text{ km s}^{-1} \text{Mpc}^{-1}$.

remark also applies to the results from BAO data combined with SN Ia data from JLA by L’Huillier & Shafieloo (2016), who obtain $H_0 = 68.49 \pm 1.53$. On the basis of 28 measurements of the Hubble parameter $H(z)$ analyzed by Farooq & Ratra (2013), Chen et al. (2016) also support a low value of $H_0 = 68.3 (+2.7, -2.6)$. They show that low values of H_0 are also obtained with different assumptions for the dark energy models. The problem of the two separated groups of favored values is also emphasized by (Bernal et al. 2016), who investigate some possible ways in the early-time physics to reconcile the high values from the cosmic distance ladder with the low ones more generally found.

Fig. 8 shows the relation between the predicted H_0 and Ω_m for a reference age of 13.8 Gyr (thick black line) in the scale invariant models, and for ages differing by $\pm 5\%$, (other uncertainty limits may easily be drawn). Both the low and high values of H_0 are considered here. A value of $\Omega_m = 0.21$ corresponds to the observed $H_0 = 73 \text{ km s}^{-1} \text{ Mpc}^{-1}$, while the 5% limits lead to a range of $\Omega_m = 0.165$ to 0.26 . A value of $H_0 = 68 \text{ km s}^{-1} \text{ Mpc}^{-1}$ leads to $\Omega_m = 0.28$, the $\pm 5\%$ limits corresponding to about $\Omega_m = 0.23$ and 0.345 . Thus, the low H_0 value leads to a density parameter Ω_m in rather agreement with the current values, while the high H_0 value leads to a lower Ω_m than usually obtained.

On the whole, the conclusion we may draw here is that, even if the scale invariant theory leads to slightly different estimates of H_0 and Ω_m from those of the Λ CDM models, it leads to no significant contradiction with current estimates.

5.5. The history of the expansion

The key prediction of the basic equations of cosmological models concerns the expansion function $R(t)$ of the Universe. It has an effect on the distances and related tests as shown above, as well as on the present and past expansion rates.

5.5.1. The past rates $H(z)$ vs. redshifts z

The expansion rates $H(z)$ vs. z represent a direct and constraining test on $R(t)$ over the ages. Moreover, this test involves much higher redshifts than the classical $m - z$ diagram. In order to perform valuable tests, it is necessary that the observational data are independent on the cosmological models.

Some results on $H(z)$ are obtained by the method of the cosmic chronometer, which contains no assumption depending on a particular cosmological model (Jimenez & Loeb 2002; Simon et al. 2005; Stern et al. 2010; Moresco 2015; Moresco et al. 2016). This method is based on the simple relation

$$H(z) = -\frac{1}{1+z} \frac{dz}{dt}, \quad (75)$$

obtained from $R_0/R = 1 + z$ and the definition of $H = \dot{R}/R$. The critical ratio dz/dt is estimated from a sample of passive galaxies (with ideally no active star formation) of different redshifts and age estimates. We note, however, that the method of cosmic chronometers, although independent on the cosmological models, depends on the models of spectral evolution of galaxies, mainly based on the theory of stellar evolution. The detections of BAO in surveys of high redshift quasars also provide powerful constraints. This is in particular the case for a study based on 48 640 quasars in the redshift range of $z = 2.1$ to 3.5 by Busca et al. (2013) from the BOSS survey in the SDSS-III results. This study has been extended to encompass 137 562 quasars in the same redshift range from the BOSS data release DR11 (Delubac et al. 2015), (since the second study is an enlargement of the first one, below we only consider the second set of data). The comparisons between observations and models we perform are using the useful collection of 28 Hubble parameters $H(z)$ by Farooq & Ratra (2013) based on Simon et al. (2005), Stern et al. (2010), Moresco et al. (2012), Busca et al. (2013), Zhang et al. (2014), Blake et al. (2012) and Chuang & Wang (2013). These data are completed here by three other recent high precision results by Anderson et al. (2014), Delubac et al. (2015) and Moresco et al. (2016), they are shown in red color in Fig. 9.

It is advantageous to perform the comparisons with the ratio $H(z)/(z+1)$ as a function of z rather than with $H(z)$ vs. z , (I am indebted to the referee for this remark). The deceleration parameter q (Sect. 3.4) can be written,

$$q = -\frac{\ddot{R}R}{\dot{R}^2} = -\frac{dH}{dz} \frac{dz}{dt} \frac{1}{H^2} - 1 = \frac{dH}{dz} \frac{1+z}{H} - 1, \quad (76)$$

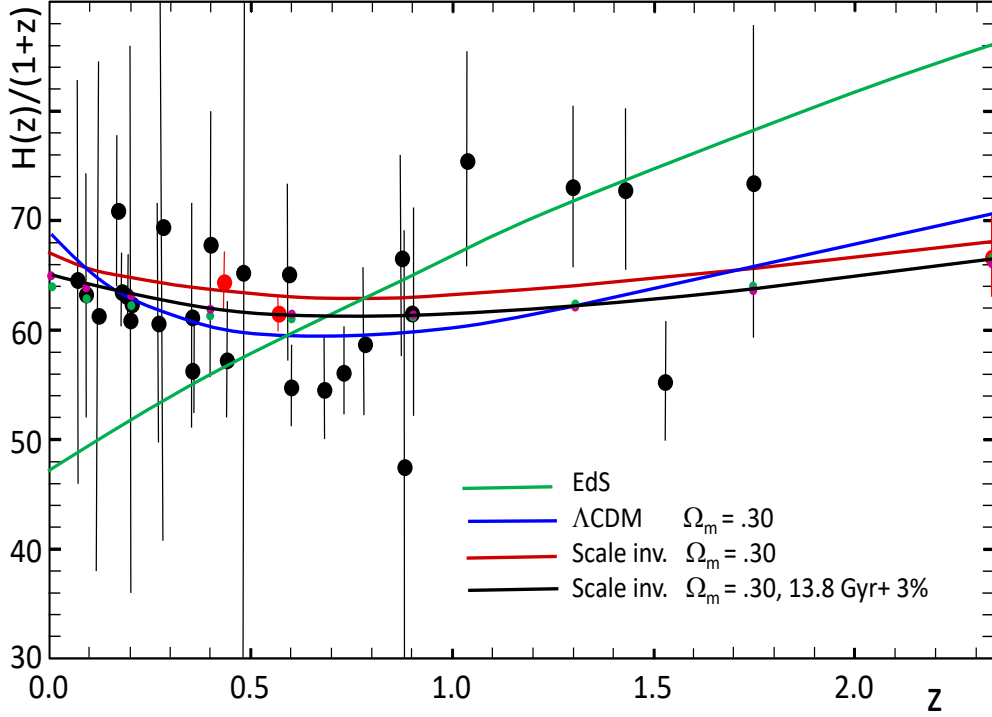


Figure 9. The plot of the $H(z)/(z+1)$ ratios vs. redshifts z with $H(z)$ in $\text{km s}^{-1} \text{Mpc}^{-1}$ reproduced from [Farooq & Ratra \(2013\)](#). The observations, represented by black dots, show the data collected by [Farooq & Ratra \(2013\)](#), with the indications of the 1σ uncertainty (see text). Three other recent values are added as red points. The red point at $z=2.34$ is from the BAO data of the BOSS DR11 quasars by [Delubac et al. \(2015\)](#), at $z=0.57$ it is from [Anderson et al. \(2014\)](#) and at $z=0.43$ from [Moresco et al. \(2016\)](#). The green line corresponds to the Einstein-de Sitter model (EdS). The blue line shows the ΛCDM for $k=0$ and $\Omega_m=0.30$ and an age of 13.8 Gyr. The red line corresponds to the best fit scale invariant model for same parameters. The black line shows the same model as the red line, but for an age 3% larger, i.e. of 14.2 Gyr.

where (75) has been used. If dH/dz decreases with increasing z , the system accelerates and consistently with (76) the q -parameter is negative. Then, the derivative

$$\frac{d}{dz} \left(\frac{H(z)}{1+z} \right) = \frac{1}{1+z} \left(\frac{dH}{dz} - \frac{H(z)}{1+z} \right) \quad (77)$$

is negative and the considered ratio is decreasing. The minimum of $H(z)/(z+1)$ is given by $\frac{dH}{dz} = \frac{H(z)}{1+z}$ which also implies that $q=0$. Thus, the minimum of the considered function occurs at the transition redshift from braking to acceleration. Then, for higher z , the braking means positive values of q and of dH/dz , implying that $H(z)/(z+1)$ is an increasing function. These properties makes $H(z)/(z+1)$ a very useful function.

Fig. 9 compares the plot of the ratios $H(z)/(z+1)$ ratios vs. z from ([Farooq & Ratra 2013](#)) and complements for various models: the Einstein-de Sitter (EdS) model, the ΛCDM and the scale invariant models for $k=0$ and $\Omega_m=0.30$. We emphasize that the results also depend on the assumed age of the Universe, since it fixes the numerical value of H_0 in $\text{km s}^{-1} \text{Mpc}^{-1}$ for the model with $H_0(\tau)=1.0$ (see Sect. 4.1). As discussed above, we generally adopt an age of 13.8 Gyr. In Fig. 9, we also show the effects for an age larger by 3% than the standard value. This corresponds to age of about 14.2 Gyr, well within the uncertainty domain of 13.8 ± 0.6 Gyr of the consensus model by [Frieman et al. \(2008\)](#). From Fig. 9, we note the following model properties:

1. For the EdS model, the continuous braking makes $H(z)/(z+1)$ to always increase and to be in clashing contradiction with the observations, especially more than the value of H_0 at $z=0$ is very low. Indeed, for this model $H_0 = (2/3)(1/t_0)$. For $t_0 = 13.8$ Gyr, we have $1/t_0 = 70.85 \text{ km s}^{-1} \text{Mpc}^{-1}$

in the considered units and taking the $2/3$ leads to $47.23 \text{ km s}^{-1} \text{ Mpc}^{-1}$. This is the well known age problem of the EdS model.

2. The values of H_0 for the Λ CDM and scale invariant models are also fixed on the basis of an age of 13.8 Gyr and of the expansion rate of the models. The facts that both models give consistent values of H_0 is a valuable point for these two models. The scale invariant model gives $H_0 = 66.9 \text{ km s}^{-1} \text{ Mpc}^{-1}$ (cf. Table 1) and the Λ CDM model $68.3 \text{ km s}^{-1} \text{ Mpc}^{-1}$, both for $k = 0$ and $\Omega_m = 0.30$.
3. The depth of the minimum of the curve $H(z)/(z + 1)$ is more pronounced for the Λ CDM model, with a difference up to about $4 \text{ km s}^{-1} \text{ Mpc}^{-1}$ compared to the scale invariant model, although the redshifts of the minimum are close to each other for $\Omega_m = 0.30$ (see Sect. 5.6).
4. For $z \geq 1.7$, the ratio $H(z)/(z + 1)$ of the Λ CDM model becomes significantly higher than for the scale invariant case. This may provide valuable tests in future.

In this context, we note that several authors have found some tension between the Λ CDM models and the $H(z)$ observations. First, [Delubac et al. \(2015\)](#) point out a 2.5σ difference at $z = 2.34$ with the predictions of a flat Λ CDM model. A strong tension is further emphasized by [Sahni et al. \(2014\)](#) and by [Ding et al. \(2015\)](#), who suggest that "allowing dark energy to evolve seems to be the most plausible approach to this problem". [Solá et al. \(2015\)](#) find a significantly better agreement with a time-evolving Λ depending on H^2 and dH/dt . The fundamental constant nature of Λ is further questioned by [Solá et al. \(2016\)](#). We will see below that the good agreement of both the Λ CDM and scale invariant models with observations lets this question open.

5.5.2. Comparisons of models and observations. The χ^2 test.

Here, we examine whether scale invariant models agree with observations and at the same time we may also see whether the claims about disagreements between observations and the Λ CDM model are further supported.

The 30 observations collected above are shown in Fig. 9 with the indications of the 1σ scatter and are compared to a few model curves. At the eye inspection, it is difficult to make a selection, apart from the EdS model. Thus, we proceed to some χ^2 tests. Firstly, we consider the Λ CDM model with $k = 0$ and $\Omega_m = 0.30$, which is of interest for comparisons with the scale invariant models below and is also very close to the best fit model by [Farooq & Ratra \(2013\)](#) with $\Omega_m = 0.29$ or 0.32 (depending on H_0). For the sample considered, we find $\chi^2 = 23.17$. If we remove the values at $z = 0.43$ and 0.57 and replace the new data at $z = 2.34$ by the former one at $z = 2.30$, our sample is the same as that by [Farooq & Ratra \(2013\)](#). It thus leads to $\chi^2 = 18.88$ which is quite consistent, owing to the slightly different Ω_m , with the minimum values of 18.24 and 19.30 found by these authors. These low χ^2 results confirm the good agreement of the Λ CDM model and observations. In Fig. 9, we also compare the flat scale invariant model with $\Omega_m = 0.30$ for an age of 13.8 Gyr to the observations. This model is, however, not the model realizing the best fit with observations. There, $\chi^2 = 26.87$, which is higher than the value of 23.17, obtained from the Λ CDM model for the same sample.

We get the best fit for models with an age higher by 3% (14.2 Gyr) than the above value. Over the range $\Omega_m = 0.30$ to 0.34 , the differences are insignificant. For $\Omega_m = 0.30$, we get $\chi^2 = 20.49$, a satisfactory value. We notice that the Λ CDM with $\Omega_m = 0.30$ appears to better reproduce the low values of $H(z)/(z + 1)$ between about $z = 0.4$ and 0.9 , while the scale invariant with the same Ω_m does better for observations with $z \geq 1.0$. This shows the great interest of future observations. However, owing to the scatter of the data, it is likely not very meaningful to enter into closer comparisons in order to disprove or support one particular model. We just conclude that the scale invariant models like the Λ CDM models, give both consistent results with the observations. Thus, scale invariant models may provide a possible alternative to the Λ CDM models and further tests are needed.

5.6. The transition redshift from braking to acceleration

We have seen in Sect. 3.5 the conditions for the occurrence of the transition from braking to acceleration which produces an inflexion point in the expansion $R(t)$. For the scale invariant model with $k = 0$, $q = 0$ occurs when $\Omega_\lambda = \Omega_m = \frac{1}{2}$. For $\Omega_m = 0.30$, the transition occurs at $R/R_0 = 0.568$ (cf. Table 1) corresponding to a transition redshift $z_{\text{trans}} = 0.76$. In the Λ CDM model, the transition lies at

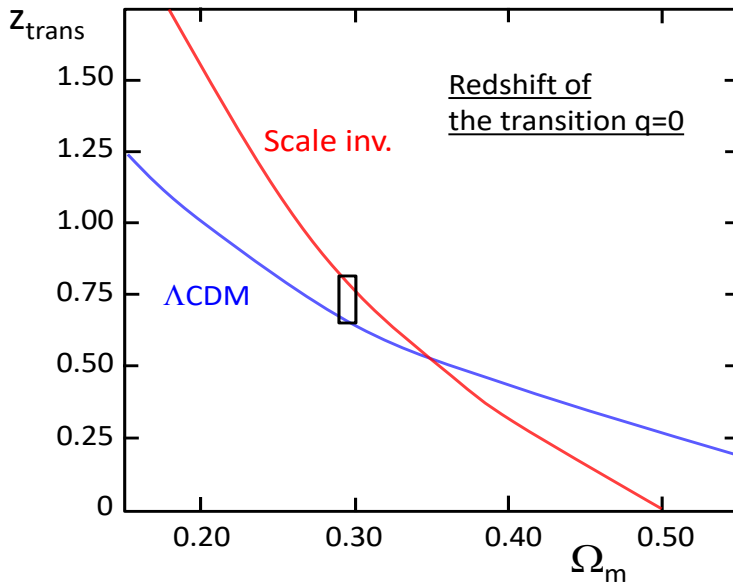


Figure 10. Relation between the redshift of the transition from braking to acceleration vs. the matter density Ω_m for the flat Λ CDM and scale invariant models. The observational values mentioned in the text are within the small black rectangle.

(Sutherland & Rothnie 2015),

$$1 + z_{\text{trans}} = \left(\frac{2\Omega_\Lambda}{\Omega_m} \right)^{1/3}, \quad (78)$$

so that for the same Ω_m , one has $z_{\text{trans}} = 0.67$, i.e. it occurs slightly later in the expansion. In both kinds of models, the transition from braking to acceleration is not a sharp one (cf. Fig. 2), the two phases being separated by a non negligible transition phase where $R(t)$ is almost linear.

Several authors have tried to estimate the value of z_{trans} . The data by Farooq & Ratra (2013), that we have extensively used above, enabled these authors to estimate a transition redshift $z_{\text{trans}} = 0.74 \pm 0.05$. This value is very well supported by other recent ones. Busca et al. (2013) gave a value of 0.82 ± 0.08 . Blake et al. (2012) found $z_{\text{trans}} \approx 0.7$, the same value is also supported by Sutherland & Rothnie (2015) and by Rani et al. (2015). The best fit by Vitenti & Penna-Lima (2015) supports a transition redshift $z_{\text{trans}} \approx 0.65$. Moresco et al. (2016) find a value $z_{\text{trans}} = 0.4 \pm 0.1$ for one model of spectral evolution and $z_{\text{trans}} = 0.75 \pm 0.15$ for another model.

Fig. 10 shows as a function of Ω_m the redshifts z_{trans} at which the transitions are located for both the Λ CDM and the scale invariant models. The value of z_{trans} varies faster with matter density for the scale invariant than for the Λ CDM case. However, the two curves are crossing at about $\Omega_m \approx 0.35$ so that they are still rather close to each other near $\Omega_m = 0.30$. The observations, which are essentially centered on the value by Farooq & Ratra (2013), extend over a range compatible with the two kinds of models. The distinction between them may be possible in the future with accurate data, for now it is still uncertain. On the whole we conclude that the observations are in good agreement with both the flat Λ CDM and scale invariant models.

6. CONCLUSIONS

The discovery of the accelerated expansion of the Universe has shown that the situation is like if an interaction of an unknown nature opposes the gravitation. In this context, the hypothesis of scale invariance, which "naturally" leads to an acceleration of the expansion, opens a window on possible interesting cosmological models. The first comparisons of models and observations made so far **on the distances, the $m - z$ diagram, the expansion rate H_0 , the dynamical properties of the scale invariant cosmology and the transition from braking to acceleration**

show consistent results. If true, the hypotheses we made have many other implications in astrophysics and cosmology.

Thus, for now these cosmological models evidently need to be further thoroughly checked with many other possible astrophysical tests in order to confirm or infirm them. In view of further tests, a point about methodology needs to be emphasized: to be valid, a test must be internally coherent and not rest on properties or inferences from the framework of other cosmological models, a point which is not always evident.

Acknowledgments: I want to express my best thanks to the physicist D. Gachet and Prof. G. Meynet for their continuous encouragements.

REFERENCES

- Anderson, L., Aubourg, E., Bailey, S. et al. 2104, MNRAS, 441, 24
- Aubourg, E., Bailey, S., Bautista, J.E. 2015, Phys. Rev. D, 92, 123516
- Bennett, C.L., Halpern, M., Hinshaw, G., Jarosik, N., Kogut, A. 2003, ApJ Suppl. 148, 1
- Bernal, J.L., Verde, L., Riess, A.G. 2016, arXiv: 1607.05617
- de Bernardis, P., Ade, P.A.R., Bock, J.J., Bond, J.L., Borrill, J. et al. 2000, Nature, 404, 955
- Bertotti, B., Balbinot, R., & Bergia, S. 1990, Modern Cosmology in Retrospect, ed. Cambridge Univ. Press.
- Betoule, M., Kessler, R., Guy, J., Mosser, J., Hardin, D. et al. 2014, Astron. Astrophys. 568, A22
- Blake, C., Brough, S., Colless, M. et al. 2012, MNRAS, 425, 405
- Bouvier, P. & Maeder, A. 1978, Ap&SS, 54, 497
- Busca, N.G., Delubac, T., Rich, J. et al. 2013, Astron. Astrophys. 552, A96
- Canuto, V., Adams, P. J., Hsieh, S.-H., & Tsiang, E. 1977, PhRvD, 16, 1643
- Carroll, S. M., Press, W. H., & Turner, E. L. 1992, ARA&A, 30, 499Cen
- Chen, G., Ratra, B. 2011, PASP, 123, 907
- Chen, Y., Kumar, S., Ratra, B. 2016, arXiv: 1606.07316
- Chuang, C.H., Wang, Y. 2013, MNRAS 455, 235
- Delubac, T., Bautista, J.E., Busca, N.G. et al. 2015, A&A, 574, A59
- Ding, X., Biesiada, M., Cao, S. et al. 2014, ApJ, 803, L22
- Dirac, P. A. M. 1973, Proceedings of the Royal Society of London Series A, 333, 403
- Eddington, A. S. 1923, The mathematical theory of relativity
- Englert, F. 2014, Ann. Phys. (Berlin) 526, 201
- Farooq, O., Ratra, B. 2013, ApJ, 766, L7
- Feng, J. L. 2010, ARA&A, 48, 495
- Feynman, R. P. 1963, Feynman lectures on physics - Volume 1
- Freedman, W. L., Madore, B. F. 2010, ARA&A, 48, 673
- Frieman, J. A., Turner, M. S., & Huterer, D. 2008, ARA&A, 46, 385
- Jimenez, R., Loeb, A. 2002, ApJ, 573, 37
- Higgs, P.W. Ann. Phys. (Berlin), 526, 211
- Hinshaw, G., Larson, D., Komatsu, E. et al. 2014, ApJ Suppl. 208, 19
- Krizek, M., Somer, L. 2016, Cosmology on Small Scales 2016, Eds. M. Krizek, Y. Dumin, Institute of Mathematics, Prague, p.65
- L'Huillier, B., Shafieloo, A. 2016, arXiv 1606.06832
- Mavrides, S. 1973, L'Univers Relativiste, Ed. Masson & Co., p. 139.
- Moresco, M. 2015, MNRAS, 450, L16
- Moresco, M., Cimatti, A., Jimenez, R. et al. 2012, J. Cosmology Astropart. Phys., 08, 006
- Moresco, M., Pozzetti, L., Cimatti, A. et al. 2016, J. Cosmology Astropart. Phys., 05, 014
- Peebles, P. J. E., Ratra, B. 1988, ApJ, 325, L17
- Peebles, P. J. E., Ratra, B. 2003, Rev. Modern Phys. 75, 559
- Perlmuter, S., Aldering, G., Goldhaber, G., et al. 1999, ApJ, 517, 565
- Planck Collaboration 2014: Ade, P. A. R. et, Aghanim, N., Armitage-Caplan, C. et al. 2014, A&A, 571, A16
- Porter, T. A., Johnson, R. P., & Graham, P. W. 2011, ARA&A, 49, 155
- Rani, N., Jain, D., Mahajan, S. et al. 2015, J. Cosmology Astropart. Phys., 12, 045
- Reid, B.A., Percival, W.J., Eisenstein, D. J. et al. 2010, MNRAS, 404, 60
- Riess, A. G., Filippenko, A. V., Challis, P., et al. 1998, AJ, 116, 1009
- Riess, A. G., Macri, L. M., Hoffmann, L.M. 2016, ApJ, 826, 56
- Sahni, V., Shafieloo, A., Starobinsky, A. A.2014, ApJ, 793, L40
- Sievers, J. L., Hlozek, R. A., Nolta, M. R. et al. 2013 JCAP, 10, 060
- Simon, J., Verde, L., Jimenez, R. 2005, PhRvD, 71, 123001
- Solà, J. 2013, Journal of Physics Conference Series, 453, 012015
- Sola, J., Gomez-Valent, A., de Cruz Perez, J. 2015, ApJ, 811, L14
- Sola, J., de Cruz Perez, J., Gomez-Valent, A., Nunes, R.C. 2016, arXiv: 1606.00450v2
- Stern, D., Jimenez, R., Verde, L., Kamionkowski, M., Stanford, S. A., 2010, J. Cosmology Astropart. Phys. 2, 008
- Sutherland, W., Rothnie, P. 2015, MNRAS, 446, 3863
- Tolman, R. C. 1934, Relativity, Thermodynamics and Cosmology, Oxford At the Clarendon Press, p.347
- Vitenti, S.D.P., Penna-Lima, M. 2015, J. Cosmology Astropart. Phys. 08, 45
- Weinberg, S. 1989, Reviews of Modern Physics, 61, 1
- Weyl, H. 1923, Raum, Zeit, Materie. Vorlesungen über allgemeine Relativitätstheorie. Re-edited by Springer Verlag, Berlin, 1970
- Zhang, C., Zhang, H., Yuan, S. et al. 2014, Research in Astron. & Astrophys., 14, 1221

ALL AUTHORS AND AFFILIATIONS

AND

ANDRE MAEDER.

Geneva Observatory, University of Geneva

CH-1290 Sauverny, Switzerland
andre.maeder@unige.ch